35th Annual International Conference of the IEEE EMBS
Osaka, Japan, 3 - 7 July, 2013

Characterization of the Spontaneous Electroencephalographic Activity in Alzheimer's Disease using Disequilibria and Graph Theory

Jesús Poza*, *Member, IEEE*, María García, *Member, IEEE*, Carlos Gómez, *Member, IEEE*, Alejandro Bachiller, Alicia Carreres, and Roberto Hornero, *Senior Member, IEEE*

Abstract— **The aim of this research was to study the changes that Alzheimer's disease (AD) elicits in the organization of brain networks. For this task, the electroencephalographic (EEG) activity from 32 AD patients and 25 healthy controls was analyzed. In a first step, a disequilibrium measure, the Euclidean distance (*ED*), was used to estimate the similarity between the spectral content of each pair of electrodes. In a second step, the similarity matrices were used to generate the corresponding graphs, from which two parameters were computed to characterize the network structure: the mean clustering coefficient and the mean path length. Results revealed significant changes ($p<0.05$) in *ED* values, as well as in the mean clustering coefficient and the mean path length, though they depend on the specific frequency band. Our findings suggest that AD is accompanied by a significant frequency-dependent alteration of brain network organization.**

I. Introduction

Alzheimer's disease (AD) is a primary neurodegenerative dementia that affects the brain cortex. Consequently, neural function is modified, reflecting the structural and functional deficits of dementia [1]. Accumulating evidence supports the notion that the analysis of electroencephalographic (EEG) activity can be a helpful tool to gain further insights into the understanding of neural dynamics [2]. Therefore, considerable effort has been devoted to explore the EEG abnormalities associated with AD [3].

Recently, modern network theory has been introduced in cognitive neuroscience to overcome the limitations of the analyses based on characterizing local activation patterns in individual sensors and functional interactions among different sensors [4]. This new framework is based upon graph theory, which is becoming a useful tool to analyze the complex organization of brain networks [5]. In this regard, the application of graph theory concepts to study AD revealed diverse neural network changes, leading to a less efficient brain function [6]–[9].

*This research was partially supported by: the *Ministerio de Economía y Competitividad* and FEDER under project TEC2011-22987; the 'Proyecto Cero 2011 on Ageing' from *Fundación General CSIC, Obra Social La Caixa* and CSIC; and, project VA111A11-2 from the *Consejería de Educación (Junta de Castilla y León)*.

J. Poza*, M. García, C. Gómez, A. Bachiller, and R. Hornero are with the Biomedical Engineering Group (GIB), Dpt. TSCIT, University of Valladolid, Paseo de Belén 15, 47011-Valladolid, Spain (phone: +34 983 423000, ext. 5569; fax: +34 983 423667; e-mail: jesus.poza@tel.uva.es).

A. Carreres is with the Hospital Universitario Pío del Río Hortega, C/Dulzaina 2, 47012-Valladolid, Spain.

The present research introduces the application of a disequilibrium measure, the Euclidean distance, to characterize the similarity patterns between the spectral content of EEG activity from different brain regions. This measure, derived from information theory, provides an alternative description of neural interactions to that offered by linear and non-linear synchronization parameters [10]. On the basis of the similarity matrix between the spectral content of sensors, a graph analysis was performed to explore the brain network structure. Hence, we wanted to address several questions: (i) does the proposed methodology based on a disequilibrium measure introduce an alternative description of neural dynamics to that provided by conventional spectral and non-linear synchronization parameters?; (ii) can the proposed methodology be useful to account for the structural network changes that AD elicits in the long-scale neural networks?

II. Materials and Methods

A. Subjects and EEG Recordings

Thirty-two patients with a diagnosis of probable AD (10 men and 22 women, age = 79.5 ± 6.5 years, mean ± standard deviation SD) and twenty-five cognitively normal volunteers (9 men and 16 women, age = 76.0 ± 7.4 years, mean ± SD) were enrolled in the study. Their cognitive function was assessed by means of the Mini-Mental State Examination (MMSE). AD patients obtained a mean MMSE score of 18.2 ± 6.7 points, whereas MMSE score for controls (CS) was 28.8 ± 1.5 points. No significant differences were observed in the mean age and gender of both groups ($p > 0.05$, Mann-Whitney U tests). All controls and patients' caregivers gave their informed consent to participate in the study. The research was approved by the local ethics committee.

Five minutes of spontaneous EEG activity were recorded from the fifty-seven participants using a digital electroencephalograph XLTEK® (Natus Medical), placed in the "Hospital Universitario Pío del Río Hortega" (Valladolid, Spain). EEG recordings were simultaneously acquired from 19 sensors distributed by the scalp according to the international 10-20 system (C3, C4, Cz, F3, F4, F7, F8, Fp1, Fp2, Fz, O1, O2, P3, P4, Pz, T3, T4, T5 and T6), with subjects in a relaxed state, awake and with their eyes closed. The sampling frequency was 200 Hz and a 50 Hz notch filter was applied to remove power line noise. Artifact-free epochs of length 5 s (26.4 ± 8.5 artifact-free epochs per channel and subject, mean ± SD) were selected for further analysis. To

complete the preprocessing step, each EEG epoch was filtered between 1 and 40 Hz.

B. Disequilibrium measure

In order to quantify the differences in the spectral content between EEG sensors, a statistical disequilibrium measure was used: the Euclidean distance (*ED*). *ED* has been previously applied to analyze the irregularity of electromagnetic brain signals [10], though it can be also defined like the distance in the probability space between two given distributions [11]. Hence, *ED* has proven useful to quantify the changes in the spectral content and, therefore, to measure the distance between two power spectra [12]. Unlike previous studies [12], in the present research we wanted to assess the role of conventional frequency bands. As a consequence, instead of computing the distance for the whole power spectra, six frequency bands were considered: δ (1-4 Hz), θ (4-8 Hz), α_1 (8-10 Hz), α_2 (10-13 Hz), β (13-30 Hz), and γ (30-40 Hz). Thus, the normalized power spectral density (PSD_n) was initially computed for each 5-s length EEG epoch (1000 samples). The normalized *ED* between the sensors *i* and *j* is then defined as [11],

$$ED_{ij}^{b}=\left\{\sum_{f\in b}\frac{\left[PSD_{n}^{i}(f)-PSD_{n}^{j}(f)\right]}{2}\right\}^{0.5},\ b=\{\delta,\theta,\alpha_1,\alpha_2,\beta,\gamma\}, \quad (1)$$

where $PSD_n^i(f)$ and $PSD_n^j(f)$ are the normalized power spectral densities for the sensors *i* and *j*, respectively; whereas, *b* denotes the conventional aforementioned frequency bands.

C. Graph Theory

A network can be represented by means of a graph, formed by a number of nodes, or vertices, and the corresponding edges between them [13]. Each edge can be weighted depending on the importance or strength of the relation between the vertices. The corresponding weights between edges can be defined using the similarity between the recorded signals in the different electrodes. In this study, the weight between two vertices *i* and *j* is computed using a distance measure (i.e. *ED*) between electrodes *i* and *j* for each frequency band. Hence, the higher the *ED* values, the lower the similarity between the spectral content of the sensors. Consequently, the *ED* values were subtracted from the unity to reflect a similarity measure [12],

$$w_{ij}^{b}=1-ED_{ij}^{b},\ b=\{\delta,\theta,\alpha_1,\alpha_2,\beta,\gamma\}. \quad (2)$$

Hence, we can define a network with N = 19 vertices (corresponding to the 19 EEG sensors), where w_{ij}^b denotes the weights between vertices for each frequency band. The generated graph can be then characterized using several parameters, though the clustering coefficient and the average path length are two fundamental features [5], [13].

The clustering coefficient measures for each vertex *i* the extent (fraction) to which its neighbors are also connected. It should be noted that symmetry is required ($w_{ij}^b = w_{ji}^b$) and $0 \le w_{ij}^b \le 1$ [8]. These constraints are fulfilled by *ED*. Therefore, the clustering coefficient for the vertex *i* and each frequency band is defined as,

$$C_i^b=\frac{\sum_{k\neq i}\sum_{\substack{l\neq i\\ l\neq k}} w_{ik}^b\cdot w_{il}^b\cdot w_{kl}^b}{\sum_{k\neq i}\sum_{\substack{l\neq i\\ l\neq k}} w_{ik}^b\cdot w_{il}^b},\ b=\{\delta,\theta,\alpha_1,\alpha_2,\beta,\gamma\}. \quad (3)$$

As shown in (3), the weights with *k*=*i*, *l*=*i* or *l*=*k* are not considered in the computation of C_i^b. In the case of isolated nodes (i.e. vertices with degree zero), all the weights w_{ij}^b are zero and the clustering coefficient takes the value $C_i^b = 0$ [8]. Finally, the average clustering coefficient for the whole graph at each frequency band is defined as,

$$C_W^b=\frac{1}{N}\cdot\sum_{i=1}^{N}C_i^b,\ b=\{\delta,\theta,\alpha_1,\alpha_2,\beta,\gamma\}. \quad (4)$$

In addition to the clustering coefficient, the average path length is a fundamental parameter to characterize a graph. It is defined as the average number of edges of the shortest path between pairs of edges. The length between two vertices *i* and *j* is defined as the inverse of the weight between them: $L_{ij}^b = 1/w_{ij}^b$ if $w_{ij}^b \neq 0$, and $L_{ij}^b = +\infty$ if $w_{ij}^b = 0$ [8]. The path length between two vertices is then defined like the sum of the lengths of the edges of this path. The shortest path l_{ij}^b between two vertices *i* and *j* is the path between *i* and *j* with the shortest length [8]. The average path length for the whole graph at each frequency band is thereby calculated as,

$$L_W^b=\frac{1}{\frac{1}{N\cdot(N-1)}\cdot\sum_{i=1}^{N}\sum_{j\neq i}^{N}\frac{1}{L_{ij}^b}},\ b=\{\delta,\theta,\alpha_1,\alpha_2,\beta,\gamma\}. \quad (5)$$

From (4) and (5), it can be seen that C_W^b is calculated using the arithmetic mean, whereas L_W^b is computed using the harmonic mean. Hence, the definition of L_W^b takes into account infinite path lengths between isolated nodes (i.e. $1/\infty \rightarrow 0$) [8].

It is noteworthy that both C_W^b and L_W^b depend on the edge weights, the network structure, and the network size. In order to achieve size-independent network parameters, they were normalized by $\left\langle C_W^{b,(surrogate)}\right\rangle$ and $\left\langle L_W^{b,(surrogate)}\right\rangle$, resulting in the mean clustering coefficient $\hat{C}_W^b = C_W^b / \left\langle C_W^{b,(surrogate)}\right\rangle$ and the mean path length $\hat{L}_W^b = L_W^b / \left\langle L_W^{b,(surrogate)}\right\rangle$ for each frequency band. $\left\langle C_W^{b,(surrogate)}\right\rangle$ and $\left\langle L_W^{b,(surrogate)}\right\rangle$ represent the averaged clustering coefficient and path length over an ensemble of 50 surrogate random networks. These networks were obtained from the original networks by randomly reshuffling the edge weights [8].

All computations were performed using the software package Matlab (version 7.14; Mathworks, Natick, MA).

D. Statistical Analysis

Initially, an exploratory data analysis was carried out. Data did not meet parametric test assumptions and thereby statistical significance was assessed by means of Mann-Whitney U tests ($\alpha = 0.05$).

Statistical analyses were carried out using the statistical software package SPSS Statistics (version 20; IBM Corp., Armonk, NY, USA).

III. Results and Discussion

In a first step, the graphs at each frequency band were calculated for each artifact-free epoch using the *ED* definition of (1). As shown in Table I, controls reached statistically significant lower *ED* values in θ (U=177.0, p=0.0003) than AD patients, whereas the opposite behavior was observed for *ED* in α_2 (U=195.5, p=0.0010) and β (U=183.0, p=0.0005). These results indicate that the distance between the PSD_n from EEG sensors for controls is lower in low frequency bands and higher in high frequency bands than for AD patients. This result suggests that AD is simultaneously associated with a decrease and an increase in the degree of similarity, depending on the analyzed frequency range. Functional connectivity analyses have also found diverse synchronization patterns at different frequency bands. Hence, AD has been associated with an increase of connectivity at low frequency bands and a decrease of synchronization at high frequency bands [3], [14]. By contrast, our results indicate that AD elicits a decrease and an increase of similarity in the spectral content at low and high frequency bands, respectively. It is clear, however, that functional connectivity patterns depend on the analyzed brain regions [14], whereas in the present research the grand-average of *ED* values was computed. Further research should be carried out to study whether the topographic patterns of *ED* at different frequency bands are related to those found in previous synchronization and connectivity studies [3], [14]. Likewise, the connectivity patterns are influenced by the synchronization parameter [15]. In this regard, the disequilibrium based on *ED* seems to provide different information about the neural dynamics in AD when compared to connectivity measures.

TABLE I. Euclidean Distance Values for each Group in the Frequency Bands that Showed Statistically Significant Results (P<0.05)

Group	Frequency band		
	θ^a	$\alpha_2{}^a$	β^a
CS	0.021 [0.014-0.031]	0.028 [0.019-0.033]	0.020 [0.017-0.028]
AD	0.040 [0.026-0.051]	0.017 [0.008-0.025]	0.015 [0.009-0.019]

a. Values are reported as median [interquartile range].

The mean clustering coefficient and the mean path length were calculated from each graph. The parameters were averaged for each subject and were statistically analyzed using Mann-Whitney U tests. Figs. 1 and 2 summarize the mean clustering coefficients and the mean path lengths at each frequency band for each group. As depicted in Fig. 1, controls obtained statistically significant higher $\hat{C}_W^{\delta}$ (U=251.0, p=0.0163) and $\hat{C}_W^{\theta}$ (U=168.5, p=0.0002) than AD patients, whereas $\hat{C}_W^{\alpha_2}$ (U=191.5, p=0.0008) and $\hat{C}_W^{\beta}$ (U=185.0, p=0.0005) were significantly lower for controls when compared to AD patients. On the other hand, Fig. 2 shows that controls reached statistically significant lower $\hat{L}_W^{\delta}$ (U=270.5, p=0.0370) and $\hat{L}_W^{\theta}$ (U=179.5, p=0.0004) values than AD patients, though $\hat{L}_W^{\alpha_2}$ (U=196.0, p=0.0010) and $\hat{L}_W^{\beta}$ (U=175.5, p=0.0003) were significantly higher for controls than for AD patients.

It is noteworthy that graphs showing a high regularity are strongly clustered and have long path lengths. On the contrary, graphs exhibiting a high degree of disorder are barely clustered and have short path lengths. They are not good candidates to describe a real system, like the human brain. Therefore, Watts and Strogatz [16] suggested a novel kind of networks, called "*small-world networks*", in which high clustering coefficients and short path lengths could be found simultaneously. Thus, small-world networks provide efficient information processing with a minimal number of connections [5]. In this regard, previous studies indicated that there exists a generalized loss of small-world characteristics in brain networks of AD patients [12]. Nevertheless, in line with previous research [6]–[9], our findings suggest that AD

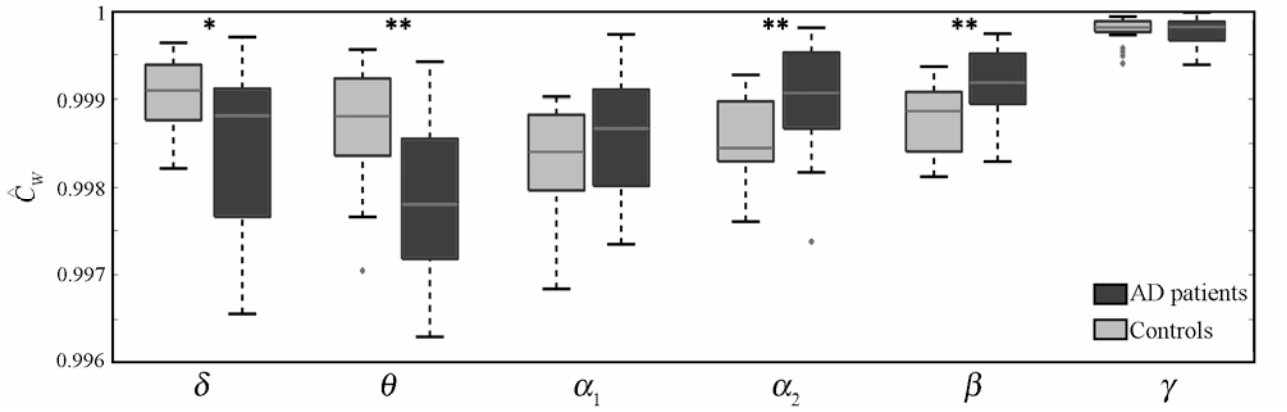

Figure 1. Boxplots displaying the differences between AD patiens and controls in mean clustering coefficients ($\hat{C}_W$) for each frequency band (δ, 1-4 Hz; θ, 4-8 Hz; α_1, 8-10 Hz; α_2, 10-13 Hz; β, 13-30 Hz; and γ , 30-40 Hz). Significant p-values are marked with asterisks (*, $p < 0.05$; **, $p < 0.01$).

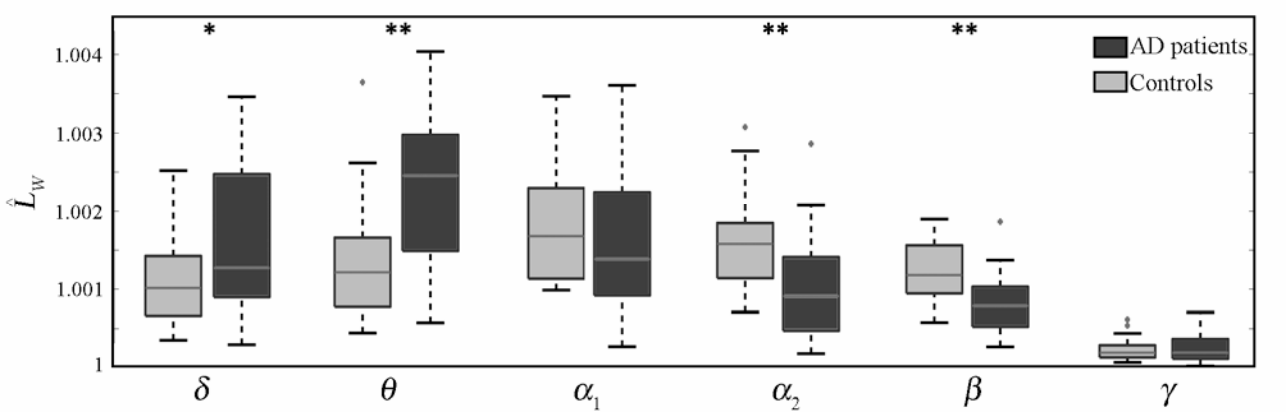

Figure 2. Boxplots displaying the differences between AD patietns and controls in mean path lengths ($\hat{L}_W$) for each frequency band (δ, 1-4 Hz; θ, 4-8 Hz; α_1, 8-10 Hz; α_2, 10-13 Hz; β, 13-30 Hz; and γ , 30-40 Hz). Significant p-values are marked with asterisks (*, $p < 0.05$; **, $p < 0.01$)

elicits a frequency-dependent alteration of the neural network organization. Specifically, the loss of small-network characteristics can be observed in low frequency bands (δ and θ), whereas high frequency bands (α_2 and β) exhibit the opposite behavior. As a consequence, the association of AD with a global loss of small-world properties might not reflect the complexity of the disease.

Finally, some aspects of the present research merit further consideration. Additional work is required to assess regional patterns of *ED* and neural network structure. Similarly, other time-frequency representations, disequilibrium measures and network parameters should be analyzed to further understand the changes that AD elicits in spontaneous EEG oscillations. Finally, it would be interesting to extend the analysis to the prodromal stage of AD (i.e., mild cognitive impairment) to achieve an early characterization of brain network abnormalities in dementia.

IV. Conclusion

Our findings support the notion that the disequilibrium between the spectral content of EEG activity from different brain regions exhibit statistically significant abnormalities in AD patients when compared to elderly controls. Furthermore, graph theory analyses suggest that AD elicits a frequency-dependent alteration of small-world network properties.

Acknowledgment

The authors would like to thank the Neurology and Neurophysiology Units from the "Hospital Universitario Pío del Río Hortega (Valladolid, Spain)" for recruiting the subjects enrolled in the present research

References

[1] J. L. Cummings, "Alzheimer's disease," *N. Eng. J. Med.*, vol. 351, pp 56–67, 2004.

[2] C. Reitz, C. Brayne, and R. Mayeux, "Epidemiology of Alzheimer Disease," *Nat. Rev. Neurol.*, vol 7, pp. 137–152, 2011.

[3] J. Jeong, "EEG dynamics in patients with Alzheimer's disease," *Clin. Neurophysiol.*, vol. 115, pp. 1490–1505, 2004.

[4] C.J. Stam and E.C. van Straaten, "The organization of physiological brain networks," *Clin. Neurophysiol.*, vol. 123, pp. 1067–1087, 2012.

[5] E. Bullmore and O. Sporns, "Complex brain networks: graph theoretical analysis of structural and functional systems," *Nat. Rev. Neurosci.*, vol. 10, pp. 186–198, 2009.

[6] W. de Haan, Y. A. L. Pijnenburg, R. L. M. Strijers, Y. van der Made, W. M. van der Flier, P. Scheltens, and C. J. Stam, "Functional neural network analysis in frontotemporal dementia and Alzheimer's disease using EEG and graph theory," *BMC Neurosci.*, vol. 10, p. 101, 2009.

[7] W. de Haan, W. M. van der Flier, T. Koene, L. L. Smits, P. Scheltens, and C. J. Stam, "Disrupted modular brain dynamics reflect cognitive dysfunction in Alzheimer's disease," *NeuroImage*, vol. 59, pp. 3085–3093, 2012.

[8] C. J. Stam, W. de Haan, A. Daffertshofer, B. F. Jones, I. Manshanden, A. M. van Cappellen van Walsum, T. Montez, J. P. A. Verbunt, J. C. de Munck, B. W. van Dijk, H. W. Berendse, and P. Scheltens, "Graph theoretical analysis of magnetoencephalographic functional connectivity in Alzheimer's disease," *Brain*, vol. 132, pp. 213–224, 2009.

[9] C. J. Stam, B. F. Jones, G. Nolte, M. Breakspear, and Ph. Scheltens, "Small-World networks and functional connectivity in Alzheimer's disease," *Cereb. Cortex*, vol. 17, pp. 92–99, 2007.

[10] R. Bruña, J. Poza, C. Gómez, A. Fernández, M. García, and R. Hornero, "Analysis of spontaneous MEG activity in mild cognitive impairment and Alzheimer's disease using spectral entropies and statistical complexity measures," *J. Neural Eng.*, vol. 9, p. 036007, 2012.

[11] R. López-Ruiz, H. L. Mancini, and X. Calbet, "A statistical measure of complexity," *Phys. Lett. A*, vol. 209, pp. 321–326, 1995.

[12] J. Poza, M. García, A. Bachiller, A. Carreres, E. Rodríguez, and R. Hornero, "Aplicación de la teoría de grafos para la caracterización de la actividad electroencefalográfica en la enfermedad de Alzheimer," presented at the *XXX Annu. Meeting Spanish Society of Biomedical Engineering*, San Sebastián, Spain, November 19–21, 2012 (in Spanish).

[13] S. Boccaletti, V. Latora, Y. Moreno, M. Chavez, and D.-U. Hwang, "Complex networks: structure and dynamics," *Phys. Rep.*, vol. 424, pp. 175–308, 2006.

[14] C. J. Stam, B. F. Jones, I. Manshanden, A. M. van Cappellen van Walsum, T. Montez, J. P. Verbunt, J. C. de Munck, B. W. van Dijk, H. W. Berendse, and P. Scheltens, "Magnetoencephalographic evaluation of resting-state functional connectivity in Alzheimer's disease," *Neuroimage*, vol. 32, pp. 1335–1344, 2006.

[15] Z. Sankari, H. Adeli, and A. Adeli, "Wavelet coherence model for diagnosis of Alzheimer disease," *Clin. EEG Neurosci.*, vol. 43, pp. 268–278, 2012.

[16] D. J. Watts and S. H. Strogatz, "Collective dynamics of 'small-world' networks," *Nature*, vol, 393, pp. 440–442, 1998.